

https://dspace.org/

Integrated renin angiotensin system dysregulation and immune profiles predict COVID19 disease severity in a South African cohort

Talitha Müller; Sonwabile Dzanibe; Cascia Day; Phelelani Mpangase; Tafadzwa Chimbetete ...

https://hdl.handle.net/10539/47356
WOS

Downloaded from a DSpace repository. https://dspace.org/

scientific reports

Check for updates

OPEN

Integrated renin angiotensin system dysregulation and immune profiles predict COVID-19 disease severity in a South African cohort

Talitha Müller[1], Sonwabile Dzanibe[2], Cascia Day[1,3], Phelelani Thokozani Mpangase[4], Tafadzwa Chimbetete[1], Sarah Pedretti[3], Sylva Schwager[5], Clive M. Gray[6], Edward Sturrock[5] & Jonny Peter[1,3]✉

Renin-angiotensin system (RAS) dysregulation is an important component of the complex pathophysiology of SARS-CoV-2 and other coronavirus infections. Thus, angiotensin-converting enzyme 2 (ACE2), the entry receptor and key to the alternative RAS, was proposed as a severity/prognostic biomarker for risk-stratification. However, experimental RAS data from diverse cohorts are limited, particularly analyses integrating RAS with immune biomarkers. Participants ($n = 172$) in Cape Town were sampled longitudinally (including a recovery timepoint [> 3-month]), across WHO asymptomatic to critical severity. Using fluorometric assays and LC-MS/MS RAS Fingerprinting®, results show serum ACE1 activity significantly decreases with increasing COVID-19 severity ($P < 0.01$) and mortality ($P < 0.05$), while increased ACE2 activity is associated with worse severity ($P < 0.01$). Neither enzyme activity correlates with viral load proxy or nasal ACE mRNA levels. ACE1 and ACE2 activities were the most effective severity biomarkers compared to 96 established immune markers obtained via proximity extension assay, as demonstrated by principal component analysis. A multivariate variable selection model using random forest classification identified biomarkers discriminating COVID-19 severity (AUC = 0.82), the strongest being HGF, EN-RAGE, cathepsin L. Adding ACE1 activity and anti-SARS-CoV-2 antibody titres improved differentiation between ambulatory and hospitalised participants. Notably, RAS dysregulation has unique severity associations in coronavirus infections with implications for treatment and pathophysiological mechanisms.

Keywords ACE2, RAS, COVID-19, MDSC, Biomarkers, SARS-CoV-2

The broad range of clinical manifestations of COVID-19 has highlighted the importance of looking beyond traditional immune mediators to understand and manage the complex pathophysiology of SARS-CoV-2 and other coronavirus infections. An important component of this broader approach unique to coronaviruses is angiotensin converting enzyme 2 (ACE2), the primary SARS-CoV entry receptor[1], which is also key to the alternative, counter-regulatory arm of the renin angiotensin system (RAS) (Fig. 1). The direction of the RAS disturbance by SARS-CoV-2 infection is debated, with early hypotheses proposing that ACE2 is downregulated due to viral entry and receptor internalisation[2], and some smaller studies finding no significant changes in RAS parameters[3]. However, recent work suggests ACE2 activity and concentration are increased in severe COVID-19[4,5], with other tissue-level data finding upregulated ACE2 expression in lung parenchyma and fluid of COVID-19 patients[6,7]. The dysregulation of the key classical RAS enzyme ACE1 is less clearly characterised, with limited data suggesting ACE1 activity is downregulated, while ACE1 concentration is poorly correlated with its

[1]Division of Allergology and Clinical Immunology, Department of Medicine, Faculty of Health Sciences, University of Cape Town, Cape Town, South Africa. [2]Division of Immunology, Institute of Infectious Disease and Molecular Medicine, University of Cape Town, Cape Town, South Africa. [3]Allergy and Immunology Unit, University of Cape Town Lung Institute, Cape Town, South Africa. [4]Sydney Brenner Institute for Molecular Bioscience, Faculty of Health Sciences, University of Witwatersrand, Johannesburg, South Africa. [5]Department of Integrative Biomedical Sciences, Institute of Infectious Disease and Molecular Medicine, Faculty of Health Sciences, University of Cape Town, Cape Town, South Africa. [6]Division of Molecular Biology and Human Genetics, Stellenbosch University, Stellenbosch, South Africa. ✉email: Jonny.Peter@uct.ac.za

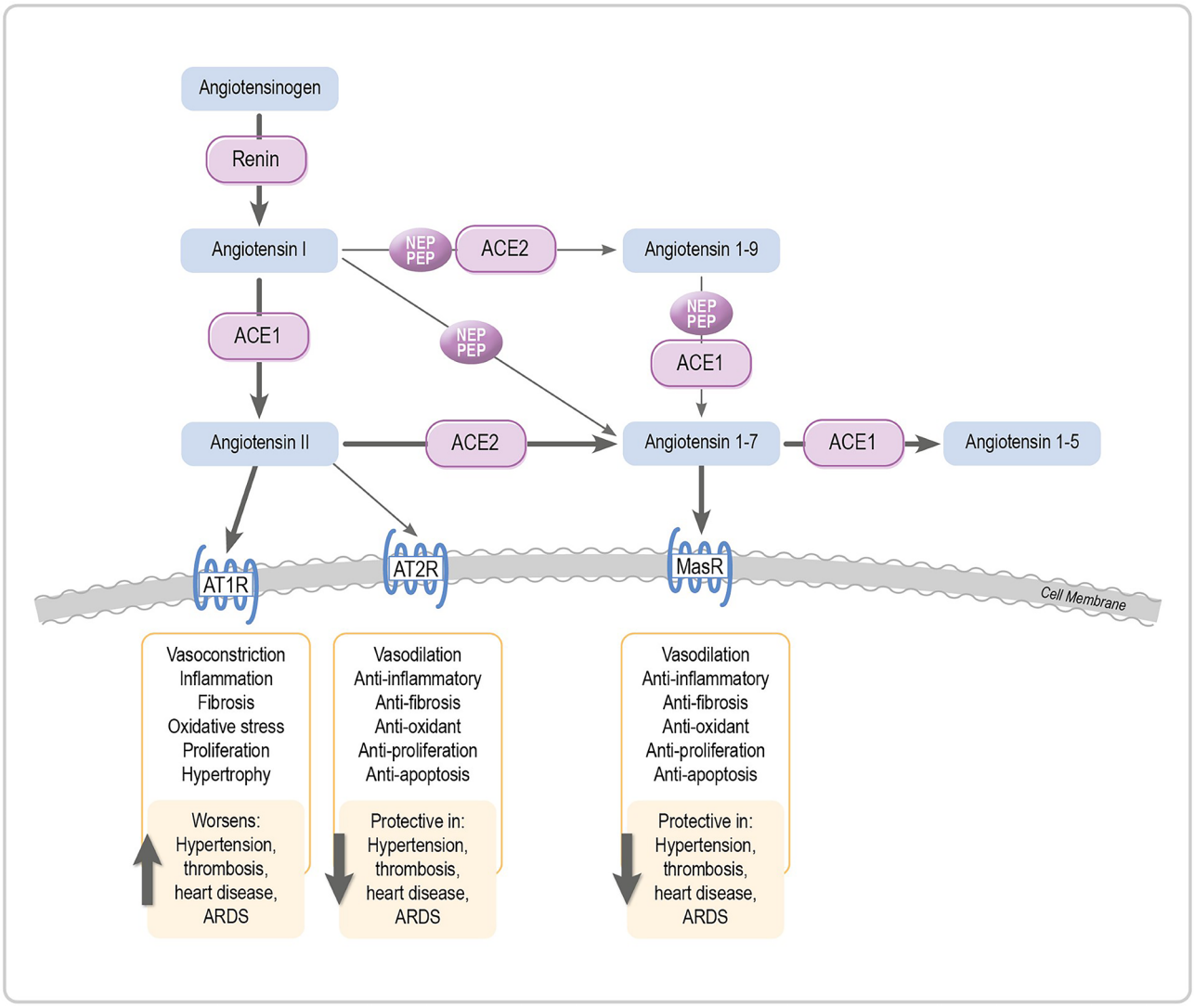


Fig. 1. A simplified schematic of the basic components of the renin angiotensin system, including the major peptides, enzymes and receptors. *ACE1* angiotensin converting enzyme 1, *ACE2* angiotensin converting enzyme 2, *ARDS* acute respiratory distress syndrome, *AT1R* angiotensin II type 1 receptor, *AT2R* angiotensin II type 2 receptor, *MasR* Mas receptor, *NEP* Neprilysin (also known as neutral endopeptidase), *PEP* prolyl endopeptidase.

activity[4,8]. Accurate study of the RAS is challenging, with several pre-analytical and analytical obstacles and thus this COVID-19 data remains limited.

As a treatment target, soluble ACE2 has been proposed as a decoy receptor and inhaled therapy continues to be studied in clinical trials[9]. Several meta-analyses of ACE inhibitors (ACEi) and angiotensin receptor blockers (ARB) indicate that continued use causes no harm and could have possible benefit in treating COVID-19[10,11]. Further therapeutic interventions targeting the RAS, particularly ACE2, may still prove essential for mitigating RAS dysregulation and disease progression in coronavirus infections, making ongoing research in this area important.

Several unanswered questions remain, including whether RAS dysregulation is an important discriminator of severity compared to well-established inflammatory markers, such as interleukin 6 (IL-6)[12], receptor for advanced glycation end-products (RAGE) and its ligand, extracellular newly identified RAGE binding protein (EN-RAGE), hepatocyte growth factor (HGF)[12], and programmed cell death ligand 1 (PD-L1)[13]. Several of these proteins suggest that a myeloid derived suppressor cell (MDSC) program is important in COVID-19 pathophysiology, which may have complex interactions with the RAS[14,15].

In this study, we investigated serum RAS profiles, integrated with 96 immune and cardiovascular biomarkers, across the spectrum of COVID-19 disease severity from asymptomatic to critical in a young South African cohort. This is the first COVID-19 cohort from Sub-Saharan Africa focused on experimental RAS data, to the best of our knowledge. Findings include that the ACE2/Ang1-7 axis is significantly increased in severe COVID-19, while the classical RAS is significantly decreased. Moreover, when modelled in the context of known

clinical and inflammatory predictors of severity, serum ACE1 and ACE2 – poorly correlated to upper airway viral loads – remain key discriminators of COVID-19 severity.

Results

Patient cohort

Adult patients with COVID-19 were recruited ($n=196$) from Groote Schuur Hospital (GSH), Cape Town, South Africa. These patients were either admitted to the COVID-19 wards, or non-hospitalised outpatients from the on-site walk-in testing centre, along with a cohort of asymptomatic healthcare workers from the Bacillus Calmette–Guérin (BCG) vaccine trial[16] ($n=29$) during 2020 and 2021. Participants with the most complete data were selected for further analysis ($n=172$) and were not different from the full set of participants (Supplementary Table S1). The selection process is fully described (Supplementary Fig. S1). Participants were recruited before COVID-19 vaccines became widely available to the public in South Africa, thus this cohort was unvaccinated. Infections occurred with SARS-CoV-2 wildtype (D614G) (33.57%), Beta (39.16%) or Delta (17.48%) variants as determined by either viral sequencing ($n=45$) or based on the dominant circulating variant during sampling[17]. The disease severity in the cohort ranged from asymptomatic to critical, according to the World Health Organisation (WHO) COVID-19 disease severity classification (Supplementary Table S2)[18]. Participants were grouped into four severity groups: asymptomatic ($n=33$), National Institute of Allergy and Infectious Diseases (NIAID) 1–2 ($n=39$) (non-hospitalised, WHO mild-moderate disease), NIAID 3–5 ($n=50$) (hospitalised, WHO moderate-severe disease), NIAID 6–7 ($n=50$) (hospitalised, WHO critical disease). Alternatively, severity was categorized as either ambulant (asymptomatic + NIAID 1–2) or hospitalised (NIAID 3–5 + NIAID 6–7) (Supplementary Table S3).

On average, there were three sampling timepoints per participant across the course of disease, and the timepoint of worst clinical severity was used for further analysis, except where otherwise stated. In addition, at a recovery timepoint 3–18 months post-disease another sample was collected ($n=98$) and/or clinical follow-up occurred. This functioned as an individualised non-illness control timepoint, particularly for RAS data. During sampling, blood, saliva and nasal scrapings were collected. Serum was used to measure RAS peptides (via mass spectrometry), enzyme activities (using fluorometric assays), immune proteomic signatures (via Olink Proximity Extension Assay) ($n=161$), and anti-spike (via ELISA) and anti-nucleocapsid antibody titres (using a cell-based assay), while nasal scrapings were used ($n=48$) to determine transcriptomic signatures at the site of disease.

The clinical characteristics of the cohort are described in Table 1. The mean age of the cohort was 47 ± 13 years, with the ambulant group (asymptomatic/NIAID 1–2) being younger than the hospitalised participants (NIAID 3–5/6–7) (35 and 44 years vs. 54 and 50 years, $P<0.001$). Hospitalised participants also had a longer duration of symptoms prior to baseline sampling compared to ambulant participants with mild disease (NIAID 1–2) (8 and 10 vs. 5 days, $P<0.001$), but the time from admission/testing to baseline sampling was not different between ambulant and hospitalised groups. Average illness duration was similar at the worst point of illness sampled, except in the critical group where the median duration and interquartile range (IQR) was longer than in other groups ($P<0.001$). There were no differences between groups in terms of body mass index (BMI) (median (IQR)): 30.5 kg/m^2 (26.4;37.0) $P=0.07$), gender (59% female (101/172), $P=0.17$) or smoking history ($P>0.1$). Participants who died made up 9.9% (17/172) of the cohort, and 30% (15/50) of the critical NIAID 6–7 group.

The most common symptoms reported were dyspnoea (68.6%, 118/172), cough (62.2%, 107/172), fever and fatigue (both 44.8%, 77/172), and myalgia (23.8%, 41/172). Significantly more NIAID 3–5/6–7 (hospitalised) participants vs. NIAID 1–2 (mild, ambulant) participants had gastrointestinal symptoms (26% and 28% vs. 8%, $P=0.045$), or dyspnoea (96% and 100% vs. 51%, $P<0.001$). More hospitalised participants than ambulant participants had hypertension (both 54% vs. 36% and 6%) or diabetes (both 40% vs. 20% and 9%) ($P<0.005$), but rates of comorbidities such as dyslipidaemia or HIV were not different. There were an increased number of participants using ACEi ($P=0.004$) or statins ($P=0.03$), respectively, but not ARB ($P=0.4$), in groups with more severe disease. Routine laboratory parameters were primarily measured in hospitalised patients and were not different between severity groups (Supplementary Tables S5 and S6). Differential counts and c-reactive protein (CRP) were not consistently ordered for COVID-19 patients at GSH (see Supplementary Methods and Supplementary Figs. S2 & S3 for management guidelines at the time)[19]. Thus, there is significant missing data for these two parameters, and to a lesser extent for D-dimer. Participant clinical characteristics were also assessed by viral variant (Supplementary Table S7) and in comparison to the subset of participants selected for Olink analysis, which were not different (Supplementary Table S8).

RAS dysregulation in COVID-19

ACE1 and ACE2 activity were measured in serum both via direct fluorometric enzyme activity assay (hereafter referred to as ACE1 activity and ACE2 activity), and via equilibrium LC-MS/MS measurement of RAS peptides (pmol/L), which were then used as a proxy for each enzyme's activity[4] and presented as a product/substrate unitless ratio (hereafter referred to as ACE-S and ALT-S, respectively).

Median ACE1 activity and ACE-S both significantly decreased ($P<0.01$ and $P<0.05$, respectively) with increasing COVID-19 severity (ACE1 activity (nmol/min/mL) – asymptomatic: 33.71 vs. NIAID 1–2: 24.7 vs. NIAID 3–5: 23.79 vs. NIAID 6–7: 18.32; ACE-S – asymptomatic: 2.66 vs. NIAID 1–2: 2.42 vs. NIAID 3–5: 1.84 vs. NIAID 6–7: 0.82) (Fig. 2a). The ACE1 activity of both asymptomatic and critical (NIAID 6–7) participants were significantly different from all other severity categories ($P<0.01$), which was also reflected by ACE-S ($P<0.05$), except that ACE-S was not significantly different between asymptomatic and NIAID 1–2 groups. This pattern remained the same when the median activity was evaluated as a fold-change normalised to the relevant parameter at each participant's recovery visit (Supplementary Fig. S5). ACE1 activity fold change was approximately 40% lower in hospitalised participants compared to asymptomatic participants, and although similar in effect size,

Characteristics	Total cohort, *n* = 172	Asymptomatic, *n* = 33	NIAID 1–2: moderate home /mild, *n* = 39	NIAID 3–5: severe/moderate hospital, *n* = 50	NIAID 6–7: critical, *n* = 50	*P*-value
Age in years, mean (sd)[b]	47 (13)	35 (11)	44 (14)	54 (10)	50 (11)	< 0.001
Female, n (%)	101 (58.7)	24 (72.7)	23 (59.0)	24 (48.0)	30 (60.0)	0.168
BMI, med (IQR)[c]	30.5 (26.4–37.0)	31.3 (26.4–36.7)	28.5 (25.3 – 33.4)	30.0 (26.4 – 35.0)	34.1 (30.5–38.4)	0.074
Smoking status						
Current smoker, n (%)	17 (10.6)	2 (6.1)	8 (22.2)	4 (8.9)	3 (6.5)	0.131
Previous smoker, n (%)[a]	23 (18.1)	NA	4 (11.1)	11 (24.4)	8 (17.4)	0.278
COVID-19 related						
Dominant variant, n (%)[a]						
Wildtype	48 (34.5)	NA	17 (43.6)	21 (42.0)	9 (18.0)	0.002
Beta	56 (40.3)	NA	6 (15.4)	22 (44.0)	26 (52.0)	
Delta	25 (18.0)	NA	11 (28.2)	5 (10.0)	8 (16.0)	
Uncertain (Beta/Delta)	14 (10.1)	NA	5 (12.8)	2 (4.0)	7 (14.0)	
Symptom duration prior to baseline sampling, days med (IQR)[a c]	7 (5–10)	NA	5 (5–7)	8 (6–10.8)	10 (7–12)	< 0.001
Days from admission, or PCR test, to baseline sampling, med (IQR)[a c]	2.5 (2–5)	NA	2 (2–4)	2 (2–4.8)	3 (1.2–5.8)	0.338
Symptom duration prior to worst sampling timepoint, days, med (IQR)[a c]	8 (6–12)	NA	7 (5–8)	8 (6–11.8)	12 (8–17)	< 0.001
Days from admission, or PCR test, to worst sampling timepoint, med (IQR)[a c]	4 (2–7)	NA	3 (2–6)	3 (2–5)	5 (3–10.5)	0.001
Symptoms, n (%)[a]						
Cough	107 (62.2)	NA	30 (76.9)	38 (76.0)	39 (78.0)	0.972
Fever	77 (44.8)	NA	19 (48.7)	27 (54.0)	31 (62.0)	0.446
Shortness of breath	118(68.6)	NA	20 (51.3)	48 (96.0)	50(100.0)	< 0.001
Fatigue	77 (44.8)	NA	28 (71.8)	24 (48.0)	25 (50.0)	0.052
Malaise[d]	13 (7.6)	NA	0 (0.0)	6 (12.0)	7 (14.0)	0.058
Myalgia[d]	41 (23.8)	NA	10 (25.6)	16 (32.0)	15 (30.0)	0.806
Headache[d]	22 (12.8)	NA	8 (20.5)	2 (4.0)	12 (24.0)	0.015
GIT symptoms[d]	30 (17.4)	NA	3 (7.7)	13 (26.0)	14 (28.0)	0.045
PaO2/FiO2 ratio, med (IQR)	141 (69–257)	NA	NA	263 (195–312)	73 (56–85)	NA
Heart rate on admission or at testing, med (IQR)[a c]	101 (82–110)	NA	73 (64–91)	105 (88–114)	102 (90–109)	0.001
Respiratory rate on admission or at testing, med (IQR)[a c]	26 (22–32)	NA	18 (18–20)	25 (22–30.2)	28 (26–34)	< 0.001
High flow nasal oxygen, n (%)	31 (18.02)	0 (0.0)	0 (0.0)	0 (0.0)	31 (62.0)	NA
Intubated, n (%)	11 (6.4)	0 (0.0)	0 (0.0)	0 (0.0)	11 (22.0)	NA
COVID-19 related death, n (%)[e]	17 (9.9)	0 (0.0)	0 (0.0)	2 (4.0)	15 (30.0)	< 0.001
Medical comorbidities						
Hypertension, n (%)	70 (40.7)	2 (6.1)	14 (35.9)	27 (54.0)	27 (54.0)	< 0.001
Diabetes Mellitus type 2 (DMT2), n (%)	51 (29.6)	3 (9.1)	8 (20.5)	20 (40.0)	20 (40.0)	0.004
Newly diagnosed, n (% of DMT2)[e]	11 (21.6)	0 (0.0)	0 (0.0)	7 (35.0)	4 (20.0)	0.160
Dyslipidaemia, n (%)[f]	14 (8.1)	0 (0.0)	3 (7.7)	4 (8.0)	7 (14.0)	0.158
Asthma, n (%)[f]	11 (6.4)	1 (3.0)	5 (12.8)	3 (6.0)	2 (4.0)	0.286
HIV, n (%)	9 (5.3)	0 (0.0)	2 (5.3)	6 (12.0)	1 (2.0)	0.060
Cardiac disease, n (%)[f]	7 (4.1)	0 (0.0)	2 (5.1)	3 (6.0)	2 (4.0)	0.507
Cancer history, n (%)[f]	9 (5.2)	1 (3.0)	2 (5.1)	6 (12.0)	0 (0.0)	0.054
Medication use, n (%)						
Continued						

Characteristics	Total cohort, $n=172$	Asymptomatic, $n=33$	NIAID 1–2: moderate home /mild, $n=39$	NIAID 3–5: severe/moderate hospital, $n=50$	NIAID 6–7: critical, $n=50$	*P*-value
ACEi	22 (12.8)	0 (0.0)	4 (10.3)	5 (10.0)	13 (26.0)	0.004
ARB	8 (4.6)	0 (0.0)	2 (5.1)	2 (4.0)	4 (8.0)	0.403
Statin	24 (14.0)	0 (0.0)	4 (10.3)	10 (20.0)	10 (20.0)	0.032
Steroids (incl. acutely)	97 (56.4)	1 (3.0)	0 (0.0)	46 (92.0)	50 (100.0)	< 0.001
NSAIDs	19 (11.0)	0 (0.0)	9 (23.1)	6 (12.0)	4 (8.0)	0.016

Table 1. Clinical characteristics of participants. Proportions reported with available data as denominator. Number of participants with available data for each characteristic indicated in Supplementary Table S4. P-values for categorical data were calculated using an N-1 (E.Pearson) Chi-squared test across all 4 severity groups (excluding total), except where otherwise stated. [a]P-value calculated excluding asymptomatic group (across the 3 remaining severity groups); data not available/excluded ($n<5$). [b]P-value calculated using ANOVA across all 4 severity groups (excluding total). [c]P-value calculated using Kruskal-Wallis test across all 4 severity groups (excluding total). [d]These symptoms were reported under the question: "Which symptoms have you experienced? Choice = Other (specify)". [e]P-value calculated using Fisher Exact Test across all 4 severity groups (excluding total). [f]These conditions were reported under the question: "Other chronic illnesses (specify)". *ACEi* ACE-inhibitor, *ARB* angiotensin receptor blocker, *BMI* body mass index, *GIT* gastrointestinal, *GIT symptoms* any of nausea and/or vomiting and/or diarrhoea, *HIV* human immuno-deficiency virus, *IQR* interquartile range, *med* median, *NA* not available, *NIAID* National Institute of Allergy and Infectious Diseases ordinal scale, *PaO2/FiO2* ratio of arterial partial pressure of oxygen to fraction of inspired oxygen, *sd* standard deviation.

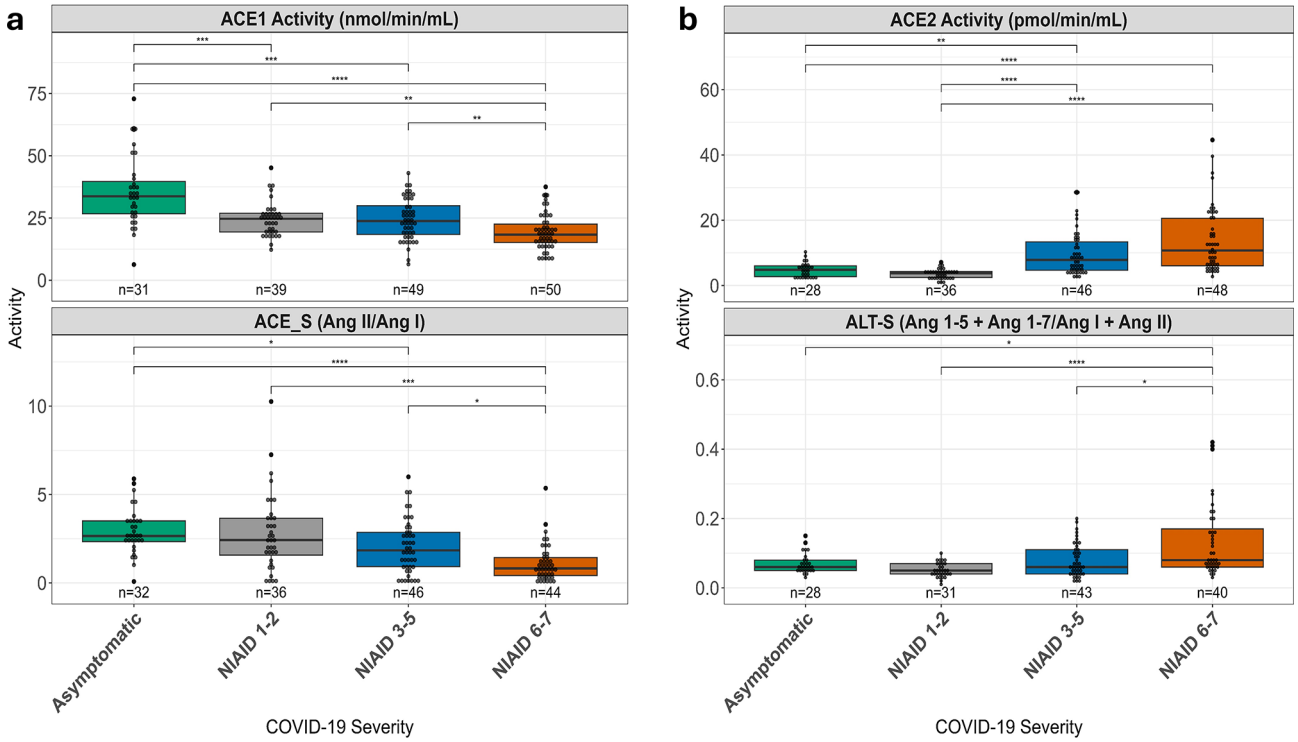


Fig. 2. Serum ACE1 and ACE2 enzyme activities are dysregulated in COVID-19 and are correlated with disease severity. (**a**) ACE1 enzyme activity and enzyme activity based on equilibrium RAS peptide (ACE-S) levels decrease significantly with COVID-19 severity. (**b**) ACE2 enzyme activity and enzyme activity based on equilibrium RAS peptide (ALT-S) levels increase significantly with COVID-19 severity; see Supplementary Figure S4 for full figure of ACE2 enzyme activity with all outliers ($n=12$) present (no change in significance). The boxplot is arranged as follows: central line for each box: median, box limits: 1st and 3rd quartiles, whiskers: 1.5x interquartile range, points beyond whiskers: outliers. p-value significance levels: ****$p<0.0001$, ***$p<0.001$, **$p<0.01$, *$p<0.05$, non-significant: not shown.

for ACE-S this was reduced to a non-significant trend after adjusting for multiple comparisons, except between asymptomatic and NIAID 3–5 groups (0.87 vs. 0.475, $P = 0.018$).

Conversely, median ACE2 activity and ALT-S both significantly increased ($P < 0.01$ and $P < 0.05$, respectively) with increasing COVID-19 severity, with the greatest differences observed between hospitalised and ambulant groups (ACE2 activity (pmol/min/mL) – asymptomatic: 4.82 vs. NIAID 1–2: 3.78 vs. NIAID 3–5: 7.86 vs. NIAID 6–7: 10.74; ALT-S – asymptomatic: 0.06 vs. NIAID 1–2: 0.05 vs. NIAID 3–5: 0.06 vs. NIAID 6–7: 0.08) (Fig. 2b). These findings were consistent when evaluating ACE2 activity and ALT-S fold change, calculated as above (Supplementary Fig. S5); ACE2 activity increased by 2.5 times (250%) in critical disease and 1.8 times (180%) in NIAID 3–5 participants compared to in the ambulant group, and ALT-S increased by 1.75 times (175%), although this parameter did not increase in moderate/severe hospitalised (NIAID 3–5) vs. ambulant participants, but rather in critical NIAID 6–7 participants. These results (for both ACE1 and ACE2 activities) were further confirmed to be consistent over the course of disease from relatively early in hospital admission, particularly as biomarkers for differentiating critical disease from non-critical COVID-19 illness (Supplementary Figs. S6 & S7). Neither ACE1 nor ACE2 activities varied in participants sampled at ≤ 7 days vs. > 7 days from symptom onset in this dataset (Supplementary Fig. S8). In addition, results were analysed across different SARS-CoV-2 variants within severity groups, but no significant differences were seen between strains (Supplementary Fig. S9).

When RAS parameters were analysed according to hypertension status (yes/no) and according to RAS-modifying drug use (i.e. ACEi/ARB), similar results were seen in non-hypertensive participants (Supplementary Fig. S10). Even in hypertensive participants, either using ACEi/ARB (Supplementary Fig. S11) or not (Supplementary Fig. S12), ACE2 activity tended to increase with increasing COVID-19 severity, but this trend was not statistically significant. ACE1 activity tended to decrease with increasing severity, but this trend disappeared in participants on ACEi/ARB. This lack of significance in hypertensive participants could be due to a much smaller sample size, especially for those on ACEi/ARB, or due to the lack of an asymptomatic comparison group, as only two of the asymptomatic participants in this cohort had hypertension and neither were using ACEi/ARB.

Gene expression was measured in nasal mucosa scrape samples and analysed for a subset of participants ($n = 48$) (Fig. 3). Neither ACE nor ACE2 mRNA levels in the nasal mucosa were significantly different between COVID-19 severities ($P = 0.327$). Furthermore, there was no correlation between serum enzyme activity and nasal mucosal scrape mRNA expression of ACE1 ($R = 0.27$, $P = 0.073$) or ACE2 (R=-0.09). There was also no correlation between ACE2 activity ($r^2 = 0.013$) nor ACE1 activity ($r^2 = 0.0005$) and SARS-CoV-2 CT value ($n = 68$, from routine diagnostic samples), respectively (Supplementary Fig. S13). Since CT value is inversely correlated with viral load[20], this indicates that RAS dysfunction is not merely a proxy for viral load, but a separate pathophysiological phenomenon in COVID-19.

Surprisingly, despite the mutual association with COVID-19 severity, neither RAS peptide parameter was highly correlated with its respective ACE enzyme activity (Supplementary Fig. S14). ACE-S was very poorly correlated to ACE1 activity in the whole cohort ($r^2 = 0.17$), and even less in subgroup analyses, except in all non-hypertensive participants ($r^2 = 0.30$) and in asymptomatic non-hypertensive participants ($r^2 = 0.41$). The correlation between ALT-S and ACE2 activity was similar ($r^2 = 0.32$).

Integrated immune and RAS signatures

To assess the importance of RAS dysregulation in COVID-19 pathophysiology compared to more well-established biomarkers, we conducted an integrated analysis of the RAS data for this cohort with serum immune proteomic data (96 proteins), which was available for most participants ($n = 161$), Fig. 4.

Principal component analysis (PCA) revealed that this integrated data discriminated clearly between severity groups (Fig. 4a), and especially between ambulant and hospitalised participants (Fig. 4c). Grouping by COVID-19 severity levels was statistically significant ($r^2 = 0.21$, $P < 0.01$) when analysed by permutational multivariate analysis of variance (PERMANOVA) with the model adjusted for time from symptom onset and sample random effects. These groups were also clearly discriminated by unsupervised cluster analysis (Fig. 4b), with cluster 2 primarily representing ambulant COVID-19 participants. The most discriminatory factors separating clusters after age were ACE2 and ACE1 activity, respectively (Fig. 4d). Other important discriminators included cathepsin L (CTSL1), which is an endosomal protease involved in SARS-CoV-2 cell entry[21], markers of MDSCs, such as PD-L1 and galectin-9 (Gal-9), and cytokines counteracting the MDSC signal, such as HGF, CUB domain-containing protein 1 (CDCP1), IL-1 receptor antagonist protein (IL-1Ra) and IL-7, as well as those counteracting key COVID-19 pathologies, such as pro-adrenomedullin (ADM). The levels of the analytes included in the PCA were visualised by heatmap using an unsupervised hierarchical clustering approach, which revealed protein groups whose levels differed between ambulant and hospitalised participants (Fig. 4e). The proteins that clearly differentiated these groups and were significantly higher in hospitalised participants include anti-SARS-CoV-2 antibody titres (anti-spike and anti-nucleocapsid), and MDSC markers, such as EN-RAGE and oncostatin-M (OSM), anti-MDSC markers, such as HGF, and cytokines contributing to key COVID-19 pathology, such as tumour necrosis factor ligand superfamily member 14 (TNFSF14). Biomarkers that were lower in hospitalised participants include TNF-related activation-induced cytokine (TRANCE, also known as RANKL), tumour necrosis factor beta (TNFB), IL-12 subunit beta (IL-12B), and neurotrophin-3 (NT-3). Interestingly, IL-8, C-C motif chemokine 3 (CCL3), and CCL4 are increased primarily in asymptomatic participants (Supplementary Table S10).

To directly test the ability of RAS and other proteomic biomarkers to define COVID-19 severity, we used a multivariate unbiased variable selection model (hereafter, multivariate severity model)[22], both with and without ACE1 and ACE2 activity and the other laboratory/clinical variables (Fig. 5). The model performed well, with a high specificity and sensitivity, particularly when discriminating between ambulatory and hospitalised participants (AUC = 0.82).

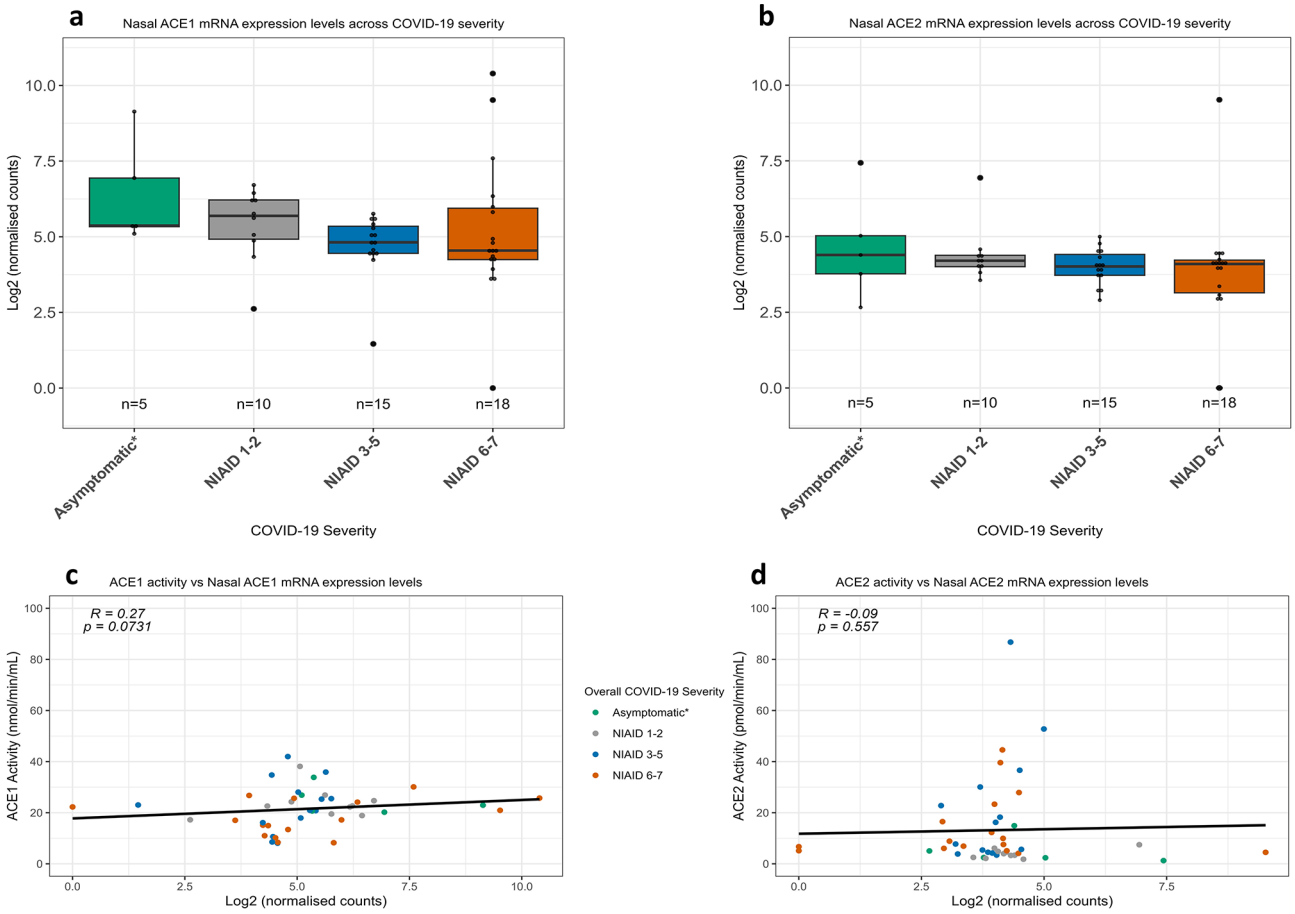


Fig. 3. ACE1 and ACE2 gene expression levels in the nasal mucosa are not significantly altered across disease severity in COVID-19, nor correlated to serum enzyme activity, in this smaller subset of the cohort. (**a**) ACE1 mRNA levels vs. COVID-19 severity at time of sampling; (**b**) ACE2 mRNA levels vs. COVID-19 severity at time of sampling; (**c**) Serum ACE1 activity lacks correlation with ACE1 gene expression in the nasal mucosa; (**d**) Serum ACE2 activity lacks correlation with ACE2 gene expression in the nasal mucosa. The boxplot is arranged as follows: central line for each box: median, box limits: 1st and 3rd quartiles, whiskers: 1.5x interquartile range, points beyond whiskers: outliers. Asymptomatic*: Includes data from asymptomatic & recovery timepoints. Correlations were calculated using Spearman's Rho. Non-significant p-values not shown.

The addition of ACE1 and ACE2 activity to the model, as well as anti-SARS-CoV-2 antibody titres, improved the ability of the model to predict severity between ambulatory and hospitalised participants, but slightly worsened the discrimination between different severity groups within the hospitalised category. Among the key proteins driving the predictive models, the top 5 proteins remained the same as the previous model. The anti-spike and anti-nucleocapsid anti-SARS-CoV-2 antibody titres as well as ACE1 activity were in the top 15 biomarkers of the second model, but ACE2 activity was not.

Many of the top immune biomarkers in these models are the same as the ones identified in the heatmap in Fig. 4e. These include markers of SARS-CoV-2 entry (CTSL1), MDSCs (EN-RAGE), markers counteracting MDSC signals (HGF, IL-7, ADM) and markers of interferon-secreting pathways (IL-12 subunit p40 (IL-12B)). While still selected, CCL3, Gal-9, OSM, IL-8, and TRANCE were less important in the predictive models compared to the PCA.

Prognostic markers

Finally, the associations with survival were evaluated (Fig. 6). This analysis was restricted to severe and critical groups, namely patients with a clear clinical risk of mortality, to avoid highlighting biomarkers for severity instead of specifically for survival (Supplementary Fig. S15 shows all severities). In this subset, ACE1 activity was significantly lower in deceased compared to survivors (median: 15.6 vs. 19.7 nmol/min/mL, $P = 0.029$), but the difference in ACE-S was not statistically significant between groups, nor was ACE2 activity or ALT-S altered. Three immune biomarkers were significantly increased in deceased participants after adjusting for multiple comparisons, namely CCL20, IL-17 C and osteoprotegerin (OPG, a decoy receptor for TRANCE). In survivors, both CD244 and chymotrypsin-C were significantly elevated.

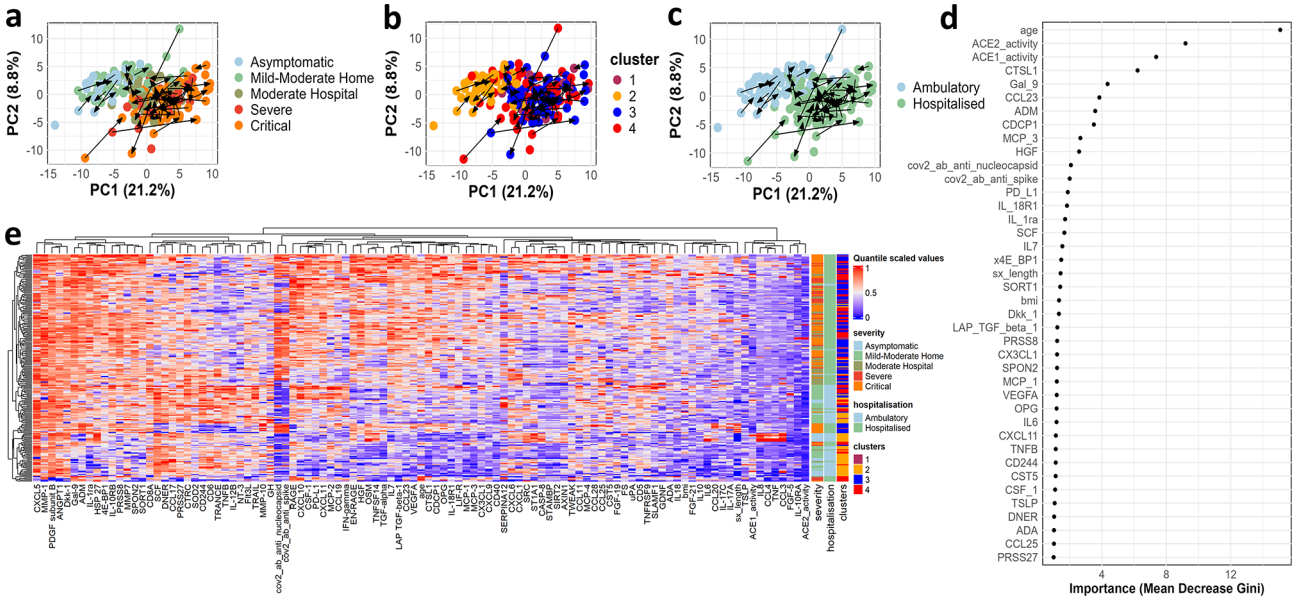


Fig. 4. Integrated immune and RAS COVID-19 severity signatures. (**a**–**c**) PCA plots of RAS enzyme activity data integrated with immune proteomic data ($n = 96$ proteins), along with anti-SARS-CoV-2 antibody titres (against spike & nucleocapsid proteins), symptom duration, age and BMI as covariates. These data were able to discriminate between COVID-19 severity groups, both when assigned and with unsupervised cluster analysis, with the models adjusted for time from symptom onset and sample random effects. (**a**) PCA discriminating COVID-19 severity groups; (**b**) PCA with unsupervised clustering; (**c**) PCA discriminating between ambulant and hospitalised groups; (**d**) Key biomarkers contributing to differences between clusters in the PCA plots. (**e**) Heatmap of the data used for the PCA plots, compared to clustering of severity groups from (**a**), PCA clusters from (**b**) and clustering of ambulant vs. hospitalised groups from (**c**). Blue-to-red colour range represents low to high relative levels of the variables. *CTSL1* cathepsin L, *Gal_9* galectin 9, *CCL23* C-C motif chemokine 23, *ADM* adrenomedullin, *CDCP1* CUB domain-containing protein 1, *MCP_3* Monocyte chemotactic protein 3, *HGF* hepatocyte growth factor, See Supplementary Table S9 for full list of proteins and Supplementary Table S10 for the full list of significantly altered biomarkers.

Discussion

Viruses cause pathology via direct cytopathy with associated tissue damage, via secondary immune damage and perturbations of normal host physiology. The SARS-CoV-2 pandemic highlighted the importance of immune-driven tissue injury, as well as the role of RAS dysregulation in viral infections, since coronavirus infections utilise ACE2 as entry receptor[1]. The preanalytical and analytical complexities of studying the RAS has meant robust data has been slow to accumulate across diverse populations, with limited attempts to integrate RAS and immune dysregulation as potentially independent drivers of COVID-19 disease severity. Our findings make important contributions by confirming that increasing ACE2 and declining ACE1 enzymatic activities (not just serum concentration) are associated with severe COVID-19, determined by both peptide equilibrium fingerprinting and enzymatic measurement. Furthermore, our data shows COVID-19 ACE1/ACE2 enzymatic dysregulation is not simply a proxy of nasal viral load or ACE1/ACE2 gene expression. Integration of RAS with immunoproteome and clinical severity predictors highlight the relevant predictive ability of particularly ACE1 decrease in COVID-19 severity and mortality.

Increased ACE2 activity was associated with increased COVID-19 severity, which is consistent with several existing studies across different populations. Fagyas et al.[23] found that increased ACE2 activity was significantly correlated with disease severity independent of comorbidities (many of which increase ACE2 activity), both in SARS-CoV-2 infection and in severe sepsis matched controls. These findings were similar in other studies[4,24], which also measured ACE2 plasma concentration, finding a strong correlation with activity[4]. A few studies have found lower or not significantly different ACE2 levels between severity groups[5,25,26]. While not all differences have clear explanations[5], main considerations for differences include: (i) small sample sizes[3,25], (ii) exclusion of key comorbidities linked to both COVID-19 severity and increased ACE2 levels[26], and (iii) problematic comparator groups including SARS-CoV-2 PCR negative controls with respiratory symptoms[26], or participants sampled late in the disease course[25]. Overall, the majority of the published literature supports an increased serum ACE2 activity and/or concentration with increasing disease severity, which normalises over several months during recovery[27].

Leading explanations for this increased serum ACE2 activity include an upregulation in tissues, as supported by single cell transcriptomic work in lungs[7] and bronchoalveolar lavage fluid (BALF)[6], and potentially increased cleavage of ACE2 from the cell surface. The mechanism of the latter could be multi-factorial including that: (i) cytokines increased in COVID-19, such as IL-1β and TNF-α, increase ACE2 shedding;[28] (ii) direct SARS-CoV

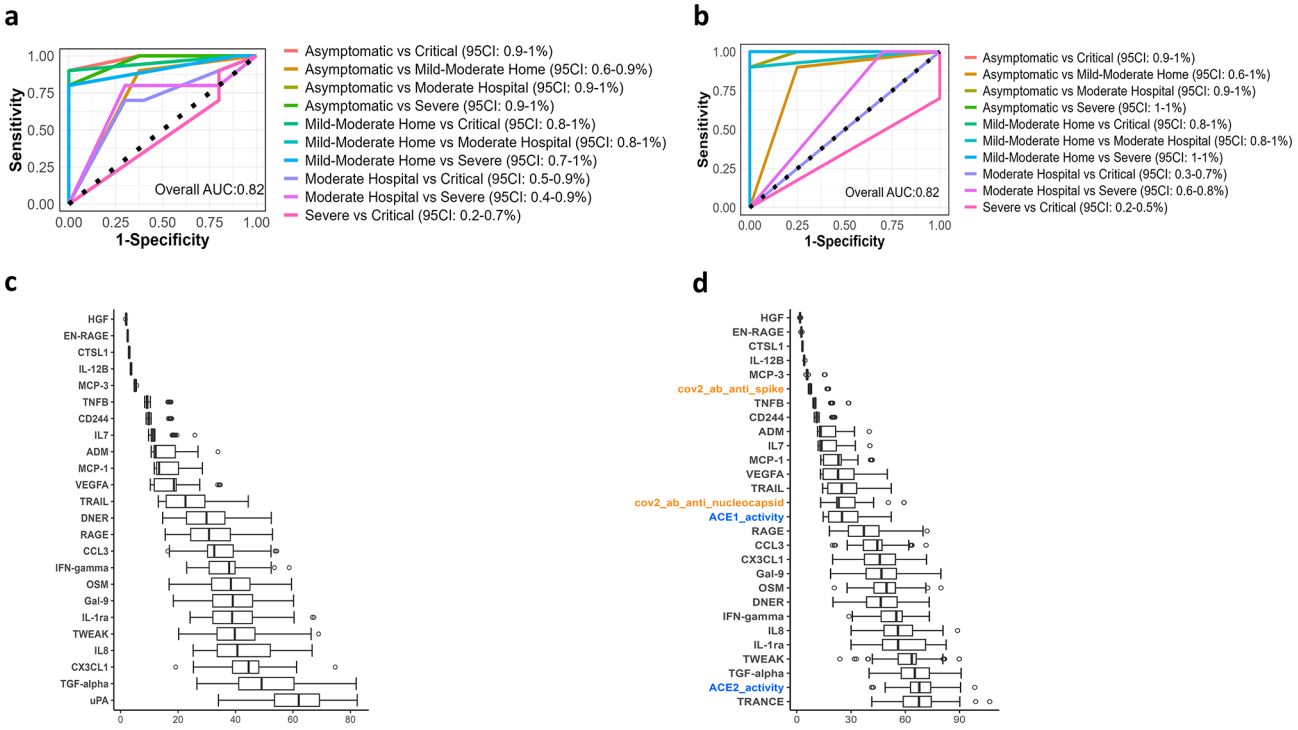


Fig. 5. Integrated immune and RAS COVID-19 severity prediction model. A multivariate unbiased variable selection model predicting COVID-19 severity, either without (**a**, **c**) or with (**b**, **d**) ACE1 and ACE2 activities and the following laboratory/clinical variables: anti-SARS-CoV-2 antibody titres (against spike & nucleocapsid proteins), age, BMI, smoking status, days from hospital admission/testing, presence of hypertension and presence of diabetes, with symptom duration included in the models as a confounding variable. The receiver operator curves (ROC) (**a**, **b**) are shown for discrimination between all possible COVID-19 severity groups in the present dataset. The most important proteins contributing to these models are shown in panels (**c**, **d**), respectively. See Supplementary Table S9 for full description of Olink biomarkers and abbreviations.

viral effects may increase shedding, as these viruses activate a disintegrin and metalloprotease 17 (ADAM17)[29], which sheds the enzymatically active ACE2 ectodomain from the cell membrane;[30] and (iii) MDSCs express ADAM17[31], and with their upregulation, may increase ACE2 shedding. Additionally, Ang II also activates ADAM17 in a local positive feedback mechanism[32]. These factors may all contribute towards the increased serum ACE2 activity observed with increasing COVID-19 severity, and need further research. In contrast to other transcriptomics studies using COVID-19 lung samples and BALF[6,7], we did not see a significant change in nasal mRNA levels of either ACE2 or ACE. While some other studies have also found no differences between severity groups[33], our findings may be the result of a limited number of nasal transcripts, or because the nasal epithelium, although part of the respiratory tract, could behave differently to lung tissue.

The dysregulation of ACE1 activity is less clearly characterised, but our findings are generally in line with the limited published experimental studies. For example, the first published study measuring ACE1 activity in COVID-19 showed that ACE1 activity was lower in 136 COVID-19 participants than in 60 healthy controls, lower in severe participants ($n = 16$), and increased at SARS-CoV-2 PCR negative follow-up[34]. These results were supported by Reindl-Schwaighofer et al.[4]. with a larger cohort ($n = 159$, $n = 680$ samples) which showed a decrease in ACE-S with increasing COVID-19 severity, similar to our results, regardless of ACEi/ARB use. The different trajectories of ACE1 activity (and ACE2 activity) between severity groups remains consistent over time, as also shown in the above cohort[4]. Further, these findings were similar to severity-matched influenza patients[4], suggesting that RAS dysregulation may not be specific to COVID-19, but rather a reflection of endothelial damage in the lungs generally, as in other causes of acute respiratory distress syndrome[35]. This could possibly explain a minority of studies that found no differences in ACE1 activity in COVID-19 when compared to other respiratory illness controls[3,36]. Furthermore, ACE1 concentration was not associated with disease severity or ACE1 activity in the above study[4]. This may be the reason why others measuring ACE1 concentration but not activity did not find it altered in COVID-19[27].

Regarding outcome data, only decreased ACE1 activity but not ACE-S or ACE2 activity were significantly associated with mortality, indicating perhaps a greater role for ACE1 dysregulation in COVID-19 pathology than ACE2. There is little data on ACE1 activity vs. mortality in the literature, but similar results were obtained when ACE-S and ALT-S alone were measured[4], in contrast to some studies focusing on ACE2 activity[23]. The unique biology of ACE1 and the RAS in African populations mean that population-specific factors may account for these discrepant findings, as well as differences in the comorbidities of COVID-19 cohorts. The immune biomarkers identified as increased in deceased participants include proteins involved in a Th17 response (IL-

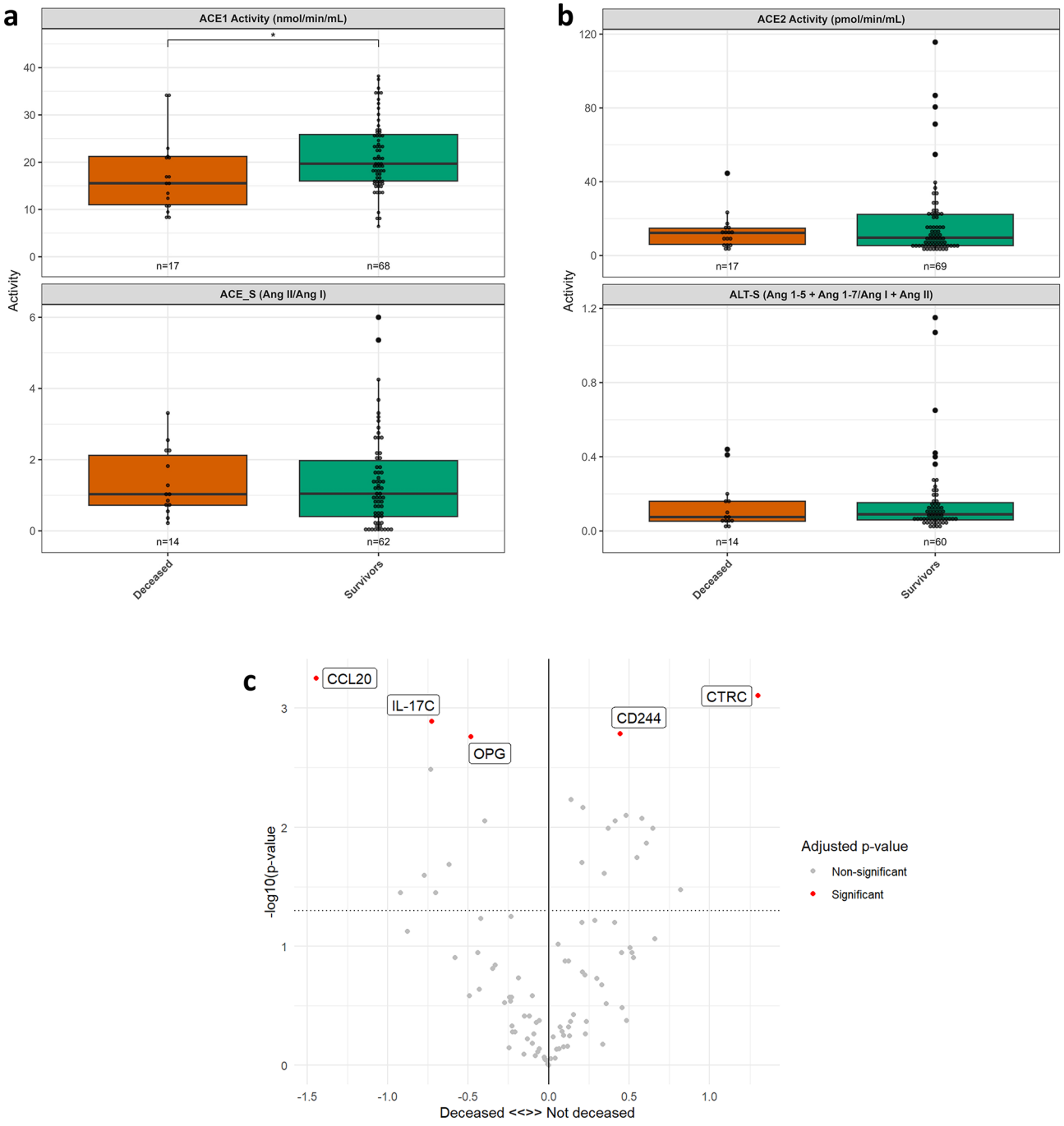


Fig. 6. Biomarkers of mortality among severe and critical patients. (**a**) ACE1 activity is significantly decreased, but not ACE-S, (**b**) nor are ACE2 activity or ALT-S significantly altered in deceased participants vs. survivors, in the context of severe/critical disease at the sampling timepoint with worst disease severity. (**c**) After adjusting for multiple comparisons, five immune biomarkers show significant differences among survivors and deceased patients. *CCL20* C-C motif chemokine 20, *CD244* cluster of differentiation 244 (Natural killer cell receptor 2B4), *CTRC* Chymotrypsin-C, *IL-17 C* interleukin 17 C, *OPG* osteoprotegerin. The boxplot is arranged as follows: central line for each box: median, box limits: 1st and 3rd quartiles, whiskers: 1.5x interquartile range, points beyond whiskers: outliers. p-value significance levels (panels (a) and (b)): *: $p < 0.05$, non-significant: not shown.

17 C, CCL20) and osteoprotegerin, which is important in osteoimmunology and gut immunosurveillance[37]. Conversely, survival markers include increased chymotrypsin-C and CD244. The latter is expressed in NK cells, T cells and MDSCs and has an immunostimulatory or -inhibitory role depending on which secondary messengers are activated[38].

There have been several studies on immune signatures in COVID-19 disease, that collectively point to early dominance of MDSCs and consequent T and NK cell suppression as important mechanisms of immune pathology[39,40]. The main immune protein discriminators between COVID-19 severity groups in our study include PD-L1, HGF, pro-adrenomedullin, CDCP1, Gal-9 and cathepsin L, which is aligned with existing literature on COVID-19 immune dysregulation[12,41,42], and with an MDSC-signature[39,43]. PD-L1 is the ligand for PD-1, an important checkpoint inhibitor[41]. PD-L1 is expressed on MDSCs, among other cell types, where it downregulates CD8 T cells' antiviral response, for example[39], and is associated with both coronavirus infection and disease progression[13,41]. In contrast, several other biomarkers counteract MDSC-associated cytokines. Particularly, HGF is involved in lung repair mechanisms, for example in pneumonia, and inhibits IL-6, IL-1β, TGF-β and IL-12, and also predicts ICU admission and death in COVID-19[12]. Pro-adrenomedullin is similarly implicated in multiple pathologies (sepsis, pneumonia, cardiac and renal disease), with pleiotropic effects, including inhibiting aldosterone and counteracting inflammation-induced endothelial permeability, thus contributing to endothelial integrity[42,44]. A recent meta-analysis showed that pro-adrenomedullin levels are significantly decreased in COVID-19 survivors[42]. Further, CDCP1 is a negative regulator of TGF-β and myofibroblasts, and has been associated with a lower risk of hospitalisation and critical COVID-19 severity[45]. In contrast, Gal-9 has a more complex interaction with the MDSC phenotype, since it contributes to activation of macrophages and polymorphs[46], but also to T cell suppression and apoptosis via its receptor – T-cell immunoglobulin- and mucin-domain-containing 3 (TIM-3)[43]. In a Canadian cohort, Gal-9 was highly elevated in severe COVID-19, and tracked with disease and recovery[46]. Finally, cathepsin L is involved in the SARS-CoV-2 endosomal entry pathway downstream of ACE2, which is an alternative to the transmembrane protease, serine 2 (TMPRSS2)-mediated cell surface entry pathway[21,47].

Three other biomarkers identified had the ability to discriminate between critical and mild disease. These include another important MDSC protein, EN-RAGE, also known as S100A12, OSM (a member of the IL-6 family), and TNFSF14, which is known to contribute to lung remodelling and fibrosis. All are associated with COVID-19 severity in other studies, in particular EN-RAGE is increased in both lung and serum samples from patients with severe COVID-19[39,40]. EN-RAGE is a damage-associated molecular pattern (DAMP) secreted by activated monocyte-macrophages and neutrophils, which induces an inflammatory response by binding RAGE in multiple inflammatory conditions, including ARDS[48,49]. It is also implicated in MDSC pathways, and has recently strongly been linked by several studies to MDSC activation in severe COVID-19[39,40,50]. Similarly, OSM is also increased in severe COVID-19 in both lung and plasma, but not peripheral blood mononuclear cells or the spleen[40,51]. OSM is a pleiotropic cytokine implicated in several other inflammatory diseases, including severe sepsis and lung fibrosis, through its roles of inducing IL-6 production, MCP-1 expression and accumulation of pro-fibrotic macrophages, for example[51–53]. Finally, other pathways highlighted in the multivariate severity model relate to a pro-inflammatory response, such as IL-12 which favours the differentiation of Th1 T cells, as well as activation of NK cells[54,55]. Synergistically with other cytokines, IL-12 stimulates release of IFN-γ via STAT4 signalling from these cells in response to viral infection[54–56]. IFN-γ causes the further secretion of IL-12 from macrophages and dendritic cells, which leads to a sustained Th1 antiviral response[55,56]. However, numerous studies have shown evidence of a defective Th1 T cell response in COVID-19, with reduced T cell activation, numbers and IFN-γ levels, with increased exhaustion markers[13,39,57]. NK cells likewise form an important part of antiviral defence, but have been shown to display lower cytotoxic and higher exhaustion markers in severe COVID-19, which is consistent with our finding of IL-12B (also known as IL-12p40) being significantly lower in hospitalised participants[57]. IL-12 itself has been associated with COVID-19 disease severity progression, in some[54] but not all[46] studies. These findings show clear evidence of immune dysregulation worsening severity.

In the combined analyses, both ACE1 and ACE2 activities remained important discriminatory factors in disease severity, with ACE1 activity in the top 15 biomarkers out of approximately 100 immunoproteome and clinical variables. Few other studies have directly compared RAS dysregulation to the coronavirus immune response. One study employed an extensive Olink panel, which included relative ACE2 amount (along with renin and renin receptor levels) and found that plasma ACE2 amounts were associated with day-28 outcomes, as well as cardiac and renal injury in intubated patients, following the late peak pattern of other endothelial injury markers[58]. However, no further comparative analysis or modelling was done between RAS and immune dysregulation biomarkers, and neither was a thorough profiling of the RAS, or even the classical arm of the RAS (e.g. ACE1), included. While several other studies compared the association between a limited number of cytokines (such as IL-6 and TNF-α) and either/both arms of the RAS[23,27], there is a paucity of substantive integrative analyses of both systems in the context of COVID-19. Therefore, the novel integrated data approach that was employed in the present study contributes towards the understanding of the meaningful role of the RAS in coronavirus pathology, even within the context of established immune dysregulation.

Lesser-known immune functions of ACE1 include effects on myeloid cells and antigen presentation, along with integrated crosstalk between RAS and MDSC signatures, with both agonistic and antagonistic effects[14]. For instance, AngII/AT1R signalling can lead to the release of IL-1β, IL-6, IL-8 and VEGF, which can all upregulate MDSC pathways[15]. However, ACE1 activity itself, through an Ang II-independent mechanism, can antagonise MDSC development in murine models[14,15]. Thus, ACE1 decrease with severe COVID-19 could either drive disease severity or be a counter-regulatory mechanism to limit MDSC-driven pathology; these effects may differ depending on the stage of viral infection. Further in vitro or animal model work is warranted to understand the implications of RAS dysregulation on current and future coronavirus disease pathology.

Our study has a few important limitations. Sampling could only be performed on or after admission/testing, thus no pre-COVID-19 samples were available for individualised baseline comparison, and the time from symptom onset could not be standardised. A further implication of this enrolment point is that the pathophysiology of disease very early on in the illness course could not be fully assessed. Nevertheless, this is generally the case in hospital-based research settings, as well as clinical care. We have tried to mitigate this effect

by including symptom duration as a confounder in the combined RAS-immunoproteome models, as well as demonstrating the utility of RAS biomarkers for differentiating disease trajectory over time. Another limitation is that recruitment occurred across three COVID-19 waves (differing viral variants). However, the consistency of the results across variants and that ACE2 remains the conserved entry receptor strengthens the case for continued relevance of the findings. Further, some subgroup sample sizes were small, particularly for ACEi/ARB treated hypertensive patients, meaning that findings are limited in these potentially relevant groups. Recruitment occurred pre-vaccine roll-out, thus this data's similarity to the vaccinated population with recurrent COVID-19 is uncertain. Moreover, the nature of our data means that only the association and not causal relationship nor the timeline between dysregulated RAS and COVID-19 severity can be delineated. Further work is required to better define these relationships and the mechanistic significance of these findings for current and future coronavirus diseases.

In conclusion, this novel integrative study has revealed promising roles for ACE2 activity as a biomarker of COVID-19 disease severity and highlighted the importance of ACE1 within the MDSC conceptual framework of coronavirus pathophysiology. Both the RAS and MDSCs are involved in a wide range of key global health concerns, including viral infections, sepsis, cardiac disease, lung fibrosis, autoimmune disease and cancer, highlighting the need for further research into both mechanistic interactions of these systems, as well as their therapeutic manipulation, including that of the alternative ACE2/Ang1-7 axis. The latter may be particularly important in conditions with a relative hypo-activation of the classical RAS, such as in coronavirus pathology.

Methods

Participant recruitment, sampling and ethics statement

Adult patients with COVID-19 (either SARS-CoV-2 PCR ($n=135$) or antigen ($n=2$) positive, or as clinically determined ($n=6$)) were recruited as soon as possible after admission or testing to the University of Cape Town (UCT) Faculty of Health Sciences (FHS) COVID-19 biorepository (HREC: R021/2020), under which sampling occurred. Patients were either admitted to Groote Schuur Hospital (GSH) or, in cases of milder disease, recruited from the GSH COVID-19 testing centre or a nearby research testing centre working in collaboration with GSH. Patients in this ACE2 sub-study were >18 years old, not pregnant and <14 days from admission (or PCR testing if not admitted) at enrolment – the vast majority were also <14 days from symptom onset; patients with known chronic kidney disease were excluded. Admissions occurred prior to COVID-19 vaccine availability in South Africa (SA) between June 2020 and July 2021, including patients across the first three waves of COVID-19 infections in SA (dominant variants: Wildtype (D614G), Beta and Delta)[17]. Data collected included demographic, clinical, and laboratory data together with blood sampling at baseline and at a median of three further sampling timepoints throughout the course of disease. The timepoint of worst clinical severity was used for further analysis, except where otherwise stated. Details of GSH and the drainage population are provided in the Supplementary Methods. A group of asymptomatic, non-hospitalised COVID-19 participants ($n=29$) from the same population were also included from the BCG Trial, full details of which are published[16]. These patients seroconverted during the course of the above study, becoming positive for SARS-CoV-2 nucleocapsid IgG antibodies and were thus selected for inclusion provided serum samples were still available. A recovery follow-up visit with sampling was attempted wherever possible for all surviving participants at least three and up to eighteen months post-discharge ($n=98$ (57%)), and at minimum mortality outcomes were followed up and recorded for all participants at this time. These studies (the biorepository; this ACE2 study; BCG trial) were approved by the UCT FHS Human Research Ethics Committee (HREC R021/2020; 257/2020; 237/2020), and all participants provided a written informed consent. All samples were anonymised and labelled with random study identifiers, and collected data was de-identified for analyses, with a separate password protected database linking patient information and study identifiers. This work was conducted in line with the principles of the Declaration of Helsinki.

Illness severity was scored based firstly on the WHO's COVID-19 disease severity classification[18], with the only modification being to evaluate the ratio of arterial partial pressure of oxygen to fraction of inspired oxygen (PaO2/FiO2) according to the National Institutes of Health (NIH)[59] and US Food and Drug Administration (FDA)[60] guidelines. Since it proved important to distinguish between ambulatory and hospitalised participants in analyses, SARS-CoV-2 infection severity was stratified into four groups according to the National Institute of Allergy and Infectious Diseases (NIAID) ordinal scale:[61] Asymptomatic nucleocapsid-serology-positive COVID-19 infected; NIAID 1–2 (ambulatory, WHO mild-moderate disease); NIAID 3–5 (hospitalised, WHO moderate-severe disease, including PaO2/FiO2 ≤ 300 and >100); NIAID 6–7 (hospitalised with WHO critical disease or PaO2/FiO2 ≤ 100). The detailed methodology for severity classification is available in the Supplementary Methods (See also Supplementary Tables S2 and S3).

Routine and specialised laboratory data and methods

Participants enrolled in the context of the UCT FHS COVID-19 biorepository did not have protocol specified blood sampling or laboratory testing; however standard-of-care at GSH for COVID-19 in-patients[19] meant that basic blood parameters available for hospitalised patients in this cohort include baseline full blood counts, electrolytes and renal function, d-dimer and occasionally CRP. Serum samples were collected for each timepoint (see Supplementary Methods) and used for the Olink Target 96 Inflammatory and Cardiovascular II proteomic panels (Supplementary Fig. S16 shows the correlation between panels). The RAS was profiled in serum using both RAS Fingerprinting® (Attoquant Diagnostics) via liquid chromatography with tandem mass spectrometry (LC-MS/MS)[62], and via measurement of ACE1 and ACE2 enzyme activities using fluorometric assays. Nasal mucosal scrapes were collected at all timepoints for participants from the Beta COVID-19 wave onwards. Anti-nucleocapsid and anti-spike IgG titres were measured using a cell-based assay and enzyme-linked immunosorbent assay (ELISA), respectively, as previously published[63]. All laboratory work received approval

from the UCT Institutional Biosafety Committee prior to conducting work. See Supplementary Methods for the full detailed laboratory methods.

Statistical analysis

Clinical and routine laboratory data were entered and stored on the secure Research Electronic Data Capture repository (REDCap, version 12.0.19, Vanderbilt University, Nashville, Tenn.). Data was then de-identified and extracted into comma-separated value files for analysis. Openware R (versions 4.0.2, 4.2.3 and 4.3.1) was used for statistical analyses and data visualisation in this study. Continuous data were summarised as medians and IQR if not normally distributed, otherwise as mean and standard deviation. Statistical differences were tested between groups using Wilcoxon rank test (non-parametric data) or t-test of mean difference (parametric data) and across groups using Kruskal-Wallis test or one-way ANOVA. Categorical data are summarised as frequencies and proportions and statistical differences tested using N-1 (E.Pearson) Chi-squared test or Fisher-exact test. A p-value of < 0.05 was considered statistically significant.

Transcriptomic data

The nf-rnaSeqCount Nextflow workflow (https://github.com/phelelani/nf-rnaSeqCount) was used to process the raw RNA-seq reads for differential expression analyses. Briefly, the quality of the raw RNA-seq FASTQ files was assessed using FASTQC and MultiQC packages. The RNA-seq reads were then aligned to the human GRCh38 reference genome using STAR to identify genomic features, and HTSeqCounts used to quantify the abundance of the identified features. The resulting raw read count matrix was used for the differential expression analysis in R (v4.4.0) using the DEseq2 package. Raw read counts were normalised using DEseq2 and $\log_2$ transformed. We compared ACE1 and ACE2 enzyme activity with log2 normalised counts across the different COVID-19 disease severity. We also compared the correlation between the enzyme activity and $\log_2$ normalised counts for ACE and ACE2 using Spearman's correlation.

Olink proteomic data

Patients' serum proteomics were quantified using the O-link proximity extension assay and presented as $\log_2$ normalized protein expression (NPX) scores. A total of 96 proteins from the Inflammation and Cardiovascular II panels were utilised, while those whose NPX values were either missing or below the limit of detection (LOD) in $> 50\%$ of the samples were excluded from further analysis (Supplementary Table S11). The remaining protein analytes whose NPX values were below LOD were either replaced with √LOD or imputed using maximum-likelihood estimates form the nrom2 R package. There were 7 proteins quantified in both of the two panels, which were highly correlated (Supplementary Fig. S16), and thus the analytes of the panels were merged. The average NPX values for the 8 samples used for Olink batch correction was used. PCA of the NPX scores for each sample was performed using the prcomp R function for dimensional reduction and visualized using the ggplot2 R package. PERMANOVA, using Euclidean distances, available in the vegan R package was used to determine the differences in the samples based on COVID-19 severity with the model adjusted for patient symptom length and sample random effects. Quantile scaled values of NPX scores, RAS data and antibody titres for each study participant was visualised using a heatmap with unsupervised hierarchical clustering from the ComplexHeatmap R package. K-mean clustering was applied for unsupervised grouping of samples based on protein NPX scores, while random forest classification, using the randomForest R package, was used to determine key variables driving the clustering. Pairwise comparisons were performed using Wilcoxon rank test and computed p-values were corrected for multiple comparisons using false discovery rates (FDR). Adjusted p-values of < 0.05 were considered statistically significant. Supplementary Table S12 contains a list of programming packages used.

Data availability

De-identified data will be made available upon reasonable request to the corresponding author.

Received: 11 October 2024; Accepted: 26 March 2025
Published online: 14 April 2025

References

1. Hoffmann, M. et al. SARS-CoV-2 cell entry depends on ACE2 and TMPRSS2 and is blocked by a clinically proven protease inhibitor. *Cell* **181**, 271–280e278. https://doi.org/10.1016/j.cell.2020.02.052 (2020).
2. Nicolau, L. A. D., Magalhaes, P. J. C. & Vale, M. L. What would Sérgio Ferreira say to your physician in this war against COVID-19: how about the Kallikrein/kinin system? *Med. Hypotheses.* **143**, 109886. https://doi.org/10.1016/j.mehy.2020.109886 (2020).
3. Kintscher, U. et al. Plasma angiotensin peptide profiling and ACE (angiotensin-converting enzyme)-2 activity in COVID-19 patients treated with Pharmacological blockers of the renin-angiotensin system. *Hypertension* **76**, e34–e36. https://doi.org/10.1161/hypertensionaha.120.15841 (2020).
4. Reindl-Schwaighofer, R. et al. The systemic renin-angiotensin system in COVID-19. *Sci. Rep.* **12**, 20117. https://doi.org/10.1038/s41598-022-24628-1 (2022).
5. Amezcua-Guerra, L. M. et al. The prognostic importance of the angiotensin II/angiotensin-(1–7) ratio in patients with SARS-CoV-2 infection. *Ther. Adv. Respir Dis.* **16**, 17534666221122544. https://doi.org/10.1177/17534666221122544 (2022).
6. Garvin, M. R. et al. A mechanistic model and therapeutic interventions for COVID-19 involving a RAS-mediated Bradykinin storm. *Elife* **9**, e59177. https://doi.org/10.7554/eLife.59177 (2020).
7. Wang, S. et al. A single-cell transcriptomic landscape of the lungs of patients with COVID-19. *Nat. Cell. Biol.* **23**, 1314–1328. https://doi.org/10.1038/s41556-021-00796-6 (2021).
8. Pucci, F., Annoni, F., Dos Santos, R. A. S., Taccone, F. S. & Rooman, M. Quantifying renin-angiotensin-system alterations in COVID-19. *Cells* **10**, 2755. https://doi.org/10.3390/cells10102755 (2021).
9. Bauer, M. et al. Phase I dose-escalation study to assess the safety, tolerability, pharmacokinetics and pharmacodynamics of an inhaled Recombinant human ACE2. *ERJ Open. Res.* **10**, 00567–02023. https://doi.org/10.1183/23120541.00567-2023 (2024).

10. Baral, R. et al. Association between renin-angiotensin-aldosterone system inhibitors and clinical outcomes in patients with COVID-19: A systematic review and meta-analysis. *JAMA Netw. Open.* **4**, e213594. https://doi.org/10.1001/jamanetworkopen.2021.3594 (2021).
11. Lee, M. M. Y. et al. Effects of renin-angiotensin system blockers on outcomes from COVID-19: A systematic review and meta-analysis of randomized controlled trials. *Eur. Heart J. Cardiovasc. Pharmacother.* **10**, 68–80. https://doi.org/10.1093/ehjcvp/pvad067 (2024).
12. Perreau, M. et al. The cytokines HGF and CXCL13 predict the severity and the mortality in COVID-19 patients. *Nat. Commun.* **12**, 4888. https://doi.org/10.1038/s41467-021-25191-5 (2021).
13. Diao, B. et al. Reduction and functional exhaustion of t cells in patients with coronavirus disease 2019 (COVID-19). *Front. Immunol.* **11**, 827. https://doi.org/10.3389/fimmu.2020.00827 (2020).
14. Bernstein, K. E. et al. Classical and nonclassical effects of angiotensin-converting enzyme: how increased ACE enhances myeloid immune function. *J. Biol. Chem.* **300**, 107388. https://doi.org/10.1016/j.jbc.2024.107388 (2024).
15. Pinter, M. & Jain, R. K. Targeting the renin-angiotensin system to improve cancer treatment: implications for immunotherapy. *Sci. Transl Med.* **9**, eaan5616. https://doi.org/10.1126/scitranslmed.aan5616 (2017).
16. Upton, C. M. et al. Safety and efficacy of Bcg re-vaccination in relation to COVID-19 morbidity in healthcare workers: A double-blind, randomised, controlled, phase 3 trial. *EClinicalMedicine* **48**, 101414. https://doi.org/10.1016/j.eclinm.2022.101414 (2022).
17. National Institute of Communicable Diseases. Data from sequencing and variant typing of laboratory confirmed cases of COVID-19 patients enrolled in syndromic surveillance for respiratory illness in South Africa, March 2020–September 2021. *Commun. Dis. Commun.* **20**, 3–4. https://www.nicd.ac.za/wp-content/uploads/2021/09/Data-from-sequencing-and-variant-typing-of-laboratoryconfirmed-cases-of-COVID-19-patients-enrolled-in-syndromic-surveillance-for-respiratory-illness-in-South-Africa-March-2020-September-2021.pdf (2021).
18. World Health Organization. *Clinical Management of COVID-19: Interim Guidance, 27 May 2020* (World Health Organization, 2020). https://iris.who.int/handle/10665/332196
19. Mendelson, M. et al. Clinical management of COVID-19: experiences of the COVID-19 epidemic from Groote Schuur hospital, cape town, South Africa. *S Afr. Med. J.* **110**, 973–981. https://doi.org/10.7196/samj.2020.v110i10.15157 (2020).
20. Rabaan, A. A. et al. Viral dynamics and real-time RT-PCR CT values correlation with disease severity in COVID-19. *Diagnostics (Basel).* **11**, 1091. https://doi.org/10.3390/diagnostics11061091 (2021).
21. Willett, B. J. et al. SARS-CoV-2 Omicron is an immune escape variant with an altered cell entry pathway. *Nat. Microbiol.* **7**, 1161–1179. https://doi.org/10.1038/s41564-022-01143-7 (2022).
22. Shi, L., Westerhuis, J. A., Rosén, J., Landberg, R. & Brunius, C. Variable selection and validation in multivariate modelling. *Bioinformatics* **35**, 972–980. https://doi.org/10.1093/bioinformatics/bty710 (2019).
23. Fagyas, M. et al. Circulating ACE2 activity predicts mortality and disease severity in hospitalized COVID-19 patients. *Int. J. Infect. Dis.* **115**, 8–16. https://doi.org/10.1016/j.ijid.2021.11.028 (2022).
24. Akin, S. et al. A low aldosterone/renin ratio and high soluble ACE2 associate with COVID-19 severity. *J. Hypertens.* **40**, 606–614. https://doi.org/10.1097/HJH.0000000000003054 (2022).
25. Osman, I. O. et al. Expression of ACE2, soluble ACE2, angiotensin I, angiotensin II and angiotensin-(1–7) is modulated in COVID-19 patients. *Front. Immunol.* **12**, 625732. https://doi.org/10.3389/fimmu.2021.625732 (2021).
26. Parikh, N. I. et al. Hospitalized patients with COVID-19 have higher plasma aldosterone-renin ratio and lower ACE activity than controls. *J. Endocr. Soc.* **6**, bvac144. https://doi.org/10.1210/jendso/bvac144 (2022).
27. Lundström, A. et al. Soluble angiotensin-converting enzyme 2 is transiently elevated in COVID-19 and correlates with specific inflammatory and endothelial markers. *J. Med. Virol.* **93**, 5908–5916. https://doi.org/10.1002/jmv.27144 (2021).
28. Jia, H. P. et al. Ectodomain shedding of angiotensin converting enzyme 2 in human airway epithelia. *Am. J. Physiol. Lung Cell. Mol. Physiol.* **297**, L84–96. https://doi.org/10.1152/ajplung.00071.2009 (2009).
29. Haga, S. et al. Modulation of TNF-alpha-converting enzyme by the Spike protein of SARS-CoV and ACE2 induces TNF-alpha production and facilitates viral entry. *Proc. Natl. Acad. Sci. U S A.* **105**, 7809–7814. https://doi.org/10.1073/pnas.0711241105 (2008).
30. Lambert, D. W. et al. Tumor necrosis factor-convertase (ADAM17) mediates regulated ectodomain shedding of the severe-acute respiratory syndrome-coronavirus (SARS-CoV) receptor, angiotensin-converting enzyme-2 (ACE2). *J. Biol. Chem.* **280**, 30113–30119. https://doi.org/10.1074/jbc.M505111200 (2005).
31. Hanson, E. M., Clements, V. K., Sinha, P., Ilkovitch, D. & Ostrand-Rosenberg, S. Myeloid-derived suppressor cells down-regulate L-selectin expression on CD4 + and CD8 + T cells. *J. Immunol.* **183**, 937–944. https://doi.org/10.4049/jimmunol.0804253 (2009).
32. Patel, V. B., Clarke, N. & Wang, Z. Angiotensin II induced proteolytic cleavage of myocardial ACE2 is mediated by TACE/ADAM-17: A positive feedback mechanism in the RAS. *J. Mol. Cell. Cardiol.* **66**, 167–176. https://doi.org/10.1016/j.yjmcc.2013.11.017 (2014).
33. Ma, D. et al. Single-cell RNA sequencing identify SDCBP in ACE2-positive bronchial epithelial cells negatively correlates with COVID-19 severity. *J. Cell. Mol. Med.* **25**, 7001–7012. https://doi.org/10.1111/jcmm.16714 (2021).
34. Zhu, Z. et al. The potential role of serum angiotensin-converting enzyme in coronavirus disease 2019. *BMC Infect. Dis.* **20**, 883. https://doi.org/10.1186/s12879-020-05619-x (2020).
35. Krenn, K., Höbart, P., Poglitsch, M., Croizé, A. & Ullrich, R. Equilibrium angiotensin metabolite profiling in patients with acute respiratory distress syndrome indicates angiotensin-converting enzyme Inhibition. *Am. J. Respir Crit. Care Med.* **202**, 1468–1471. https://doi.org/10.1164/rccm.201912-2504LE (2020).
36. Henry, B. M. et al. Serum ACE activity and plasma ACE concentration in patients with SARS-CoV-2 infection. *Scand. J. Clin. Lab. Invest.* **81**, 272–275. https://doi.org/10.1080/00365513.2021.1926536 (2021).
37. Kimura, S. et al. Osteoprotegerin-dependent M cell self-regulation balances gut infection and immunity. *Nat. Commun.* **11**, 234. https://doi.org/10.1038/s41467-019-13883-y (2020).
38. Sun, L. et al. Advances in Understanding the roles of CD244 (SLAMF4) in immune regulation and associated diseases. *Front. Immunol.* **12**, 648182. https://doi.org/10.3389/fimmu.2021.648182 (2021).
39. Hackney, J. A. et al. A myeloid program associated with COVID-19 severity is decreased by therapeutic Blockade of IL-6 signaling. *Science* **26**, 107813. https://doi.org/10.1016/j.isci.2023.107813 (2023).
40. Arunachalam, P. S. et al. Systems biological assessment of immunity to mild versus severe COVID-19 infection in humans. *Science* **369**, 1210–1220. https://doi.org/10.1126/science.abc6261 (2020).
41. Sabbatino, F. et al. PD-L1 dysregulation in COVID-19 patients. *Front. Immunol.* **12**, 695242. https://doi.org/10.3389/fimmu.2021.695242 (2021).
42. Fialek, B. et al. Systematic review with meta-analysis of mid-regional pro-adrenomedullin (MR-proadm) as a prognostic marker in COVID-19-hospitalized patients. *Ann. Med.* **55**, 379–387. https://doi.org/10.1080/07853890.2022.2162116 (2023).
43. Elahi, S., Niki, T., Hirashima, M. & Horton, H. Galectin-9 binding to Tim-3 renders activated human CD4 + T cells less susceptible to HIV-1 infection. *Blood* **119**, 4192–4204. https://doi.org/10.1182/blood-2011-11-389585 (2012).
44. Temmesfeld-Wollbrück, B. et al. Adrenomedullin reduces vascular hyperpermeability and improves survival in rat septic shock. *Intensive Care Med.* **33**, 703–710. https://doi.org/10.1007/s00134-007-0561-y (2007).
45. Baranova, A., Luo, J., Fu, L., Yao, G. & Zhang, F. Evaluating the effects of Circulating inflammatory proteins as drivers and therapeutic targets for severe COVID-19. *Front. Immunol.* **15**, 1352583. https://doi.org/10.3389/fimmu.2024.1352583 (2024).

46. Bozorgmehr, N. et al. Galectin-9, a player in cytokine release syndrome and a surrogate diagnostic biomarker in SARS-CoV-2 infection. *mBio* **12**, e00384–e00321. https://doi.org/10.1128/mbio.00384-21 (2021).
47. Jackson, C. B., Farzan, M., Chen, B. & Choe, H. Mechanisms of SARS-CoV-2 entry into cells. *Nat. Rev. Mol. Cell. Biol.* **23**, 3–20. https://doi.org/10.1038/s41580-021-00418-x (2022).
48. Jabaudon, M. et al. Soluble forms and ligands of the receptor for advanced glycation end-products in patients with acute respiratory distress syndrome: an observational prospective study. *PLoS One*. **10**, e0135857. https://doi.org/10.1371/journal.pone.0135857 (2015).
49. Wittkowski, H. et al. Neutrophil-derived S100A12 in acute lung injury and respiratory distress syndrome. *Crit. Care Med.* **35**, 1369–1375. https://doi.org/10.1097/01.Ccm.0000262386.32287.29 (2007).
50. Chen, S. T. et al. A shift in lung macrophage composition is associated with COVID-19 severity and recovery. *Sci. Transl Med.* **14**, eabn5168. https://doi.org/10.1126/scitranslmed.abn5168 (2022).
51. Russell, C. D. et al. Tissue proteomic analysis identifies mechanisms and stages of immunopathology in fatal COVID-19. *Am. J. Respir Cell. Mol. Biol.* **66**, 196–205. https://doi.org/10.1165/rcmb.2021-0358OC (2022).
52. Ricaño-Ponce, I. et al. Characterization of sepsis inflammatory endotypes using circulatory proteins in patients with severe infection: A prospective cohort study. *BMC Infect. Dis.* **22**, 778. https://doi.org/10.1186/s12879-022-07761-0 (2022).
53. Wolf, C. L., Pruett, C., Lighter, D. & Jorcyk, C. L. The clinical relevance of OSM in inflammatory diseases: A comprehensive review. *Front. Immunol.* **14**, 239732. https://doi.org/10.3389/fimmu.2023.1239732 (2023).
54. Moll-Bernardes, R. et al. IL-10 and IL-12 (p70) levels predict the risk of COVID-19 progression in hypertensive patients: insights from the BRACE-CORONA trial. *Front. Cardiovasc. Med.* **8**, 702507. https://doi.org/10.3389/fcvm.2021.702507 (2021).
55. Trinchieri, G. Interleukin-12 and the regulation of innate resistance and adaptive immunity. *Nat. Rev. Immunol.* **3**, 133–146. https://doi.org/10.1038/nri1001 (2003).
56. Abel, A. M., Yang, C., Thakar, M. S. & Malarkannan, S. Natural killer cells: development, maturation, and clinical utilization. *Front. Immunol.* **9**, 1869. https://doi.org/10.3389/fimmu.2018.01869 (2018).
57. Li, M. et al. Elevated exhaustion levels of NK and CD8 + T cells as indicators for progression and prognosis of COVID-19 disease. *Front. Immunol.* **11**, 580237. https://doi.org/10.3389/fimmu.2020.580237 (2020).
58. Leisman, D. E. et al. Alveolar, endothelial, and organ injury marker dynamics in severe COVID-19. *Am. J. Respir Crit. Care Med.* **205**, 507–519. https://doi.org/10.1164/rccm.202106-1514OC (2022).
59. COVID-19 Treatment Guidelines Panel. *Coronavirus Disease 2019 (COVID-19) Treatment Guidelines* (National Institutes of Health, 2021). https://www.ncbi.nlm.nih.gov/books/NBK570371/pdf/Bookshelf_NBK570371.pdf
60. Center for Biologics Evaluation and Research & Center for Drug Evaluation and Research. *COVID-19: Developing Drugs and Biological Products for Treatment or prevention - guidance for Industry* (U.S. Food and Drug Administration, 2020).
61. Beigel, J. H. et al. Remdesivir for the treatment of COVID-19 — final report. *N Engl. J. Med.* **383**, 1813–1826. https://doi.org/10.1056/NEJMoa2007764 (2020).
62. Binder, C. et al. Angs (angiotensins) of the alternative renin-angiotensin system predict outcome in patients with heart failure and preserved ejection fraction. *Hypertension* **74**, 285–294. https://doi.org/10.1161/HYPERTENSIONAHA.119.12786 (2019).
63. Moyo-Gwete, T. et al. Cross-reactive neutralizing antibody responses elicited by SARS-CoV-2 501Y.V2 (B.1.351). *N Engl. J. Med.* **384**, 2161–2163. https://doi.org/10.1056/NEJMc2104192 (2021).

Acknowledgements

JP is supported by National Institutes of Health (Grant K43TW011178-01), EDCTP2 programme supported by the European Union (grant number TMA2017SF-1981) and rated-researcher support from the National Research Foundation of South Africa. TM was supported in this research in part by the National Research Foundation of South Africa, the University of Cape Town, including through the Ada and Bertie Levenstein scholarship, the Harry Crossley Foundation and the Skye Foundation. SD was supported by the Wellcome Trust International Training Fellowship (221995/Z/20/Z). Research reported in this publication was supported by the South African Medical Research Council with funds received from the South African Department of Science and Innovation. The opinions, findings, and conclusions or recommendations expressed in this publication is that of the authors and the NRF, SAMRC and DSI accept no liability whatsoever in this regard.The authors would like to thank firstly our participants, and also the following then medical students from UCT for their invaluable assistance in recruiting participants and obtaining samples: Saabira Pandy, the late Tokoloho Ramabele, Thabang Lepako, Itumeleng Msimanga, Demishka Valaitham, Chanté Dove, Alexandra Walker, Ashmika Singh, Banyana Baloyi, Iphile Shenxane, Jenna Smith, Kirsten Moody, Lauren Goliath, Liyema Mkabile, Megan Bunting, Odwa Jim, Ofentse Monnaruri, Savannah Verhage, Sewela Kganakga, Sinéad McKenna, as well as Dr Mireille Porter. In addition those who assisted with the laboratory work: Brittany du Preez, Nokukhanya Tenza, Emma Fagan, Josh Loyson; as well as data management: Tsholofelo Morole, Vathiswa Kamkam. We sincerely thank Prof Penny Moore, Dr Thandeka Moyo-Gwete and Tandile Hermanus for the SARS-CoV-2 antibody data in this cohort; as well as Dr Marko Poglitsch and Dr Oliver Domineg for the RAS Fingerprinting® data and advice. Further for valuable support in the data analysis, we thank Dr Jonathan Müller. We also thank the graphic designer Karen Adamson for the drawing of Figure 1 describing the renin angiotensin system.

Author contributions

J.P. developed the objectives and research questions. J.P., E.S., C.G., S.S. and T.M. contributed to study and experimental methodology design. T.M., T.C., S.P. and C.D. assisted with data collection and project administration. T.M. and C.D. accessed and verified the underlying study data. T.M. conducted the experiments. S.D., T.M., and P.M. performed data analysis. T.M., S.D., E.S. and J.P. contributed to data interpretation. T.M. wrote the first draft of the manuscript, with E.S. and J.P. reviewing and editing the work. All authors participated in the final revisions and approval of the manuscript. All authors contributed to the article and approved the submitted version.

Declarations

Competing interests

The authors declare no competing interests.

Additional information

Supplementary Information The online version contains supplementary material available at https://doi.org/10.1038/s41598-025-96161-w.

Correspondence and requests for materials should be addressed to J.P.

Reprints and permissions information is available at www.nature.com/reprints.

Publisher's note Springer Nature remains neutral with regard to jurisdictional claims in published maps and institutional affiliations.

Open Access This article is licensed under a Creative Commons Attribution-NonCommercial-NoDerivatives 4.0 International License, which permits any non-commercial use, sharing, distribution and reproduction in any medium or format, as long as you give appropriate credit to the original author(s) and the source, provide a link to the Creative Commons licence, and indicate if you modified the licensed material. You do not have permission under this licence to share adapted material derived from this article or parts of it. The images or other third party material in this article are included in the article's Creative Commons licence, unless indicated otherwise in a credit line to the material. If material is not included in the article's Creative Commons licence and your intended use is not permitted by statutory regulation or exceeds the permitted use, you will need to obtain permission directly from the copyright holder. To view a copy of this licence, visit http://creativecommons.org/licenses/by-nc-nd/4.0/.

© The Author(s) 2025